Design of Composite Structures for Reliability and Damage Tolerance

Report for Grant
NAG 1-2038

Period of Performance
January 1998 - April 1999

Masoud Rais-Rohani, Ph.D., P.E.
Department of Aerospace Engineering
Mississippi State University
Mississippi State, MS 39762

Phone: (601) 325-7294
Fax: (601) 325-7730
E-mail: masoud@ae.msstate.edu

Submitted to

Mechanics and Durability Branch
Mail Stop 190
NASA Langley Research Center
Hampton, VA 23681

Table of Contents

Abstract

A summary of research conducted during the first year is presented. The research objectives were sought by conducting two tasks: (1) investigation of probabilistic design techniques for reliability-based design of composite sandwich panels, and (2) examination of strain energy density failure criterion in conjunction with response surface methodology for global-local design of damage tolerant helicopter fuselage structures. This report primarily discusses the efforts surrounding the first task and provides a discussion of some preliminary work involving the second task.

1. Reliability-Based Design of Composite Sandwich Panels

A reliability-based design of a rectangular sandwich plate with anisotropic face sheets and edges elastically restrained against rotation is investigated. The plate, as shown in Fig. 1, is optimized for minimum weight subject to a reliability constraint against axial and shear buckling. The influence of reliability requirement on the optimal design is evident by comparing the results of the probabilistic design with those of a deterministic design.

The plate is modeled based on the general small-deflection theory of sandwich plates with the mean values of the in-plane buckling loads determined using the Rayleigh-Ritz method according to the procedure discussed by Marcellier and Rais-Rohani[1]. The plate design is optimized using the modified method of feasible directions in DOT[2] software.

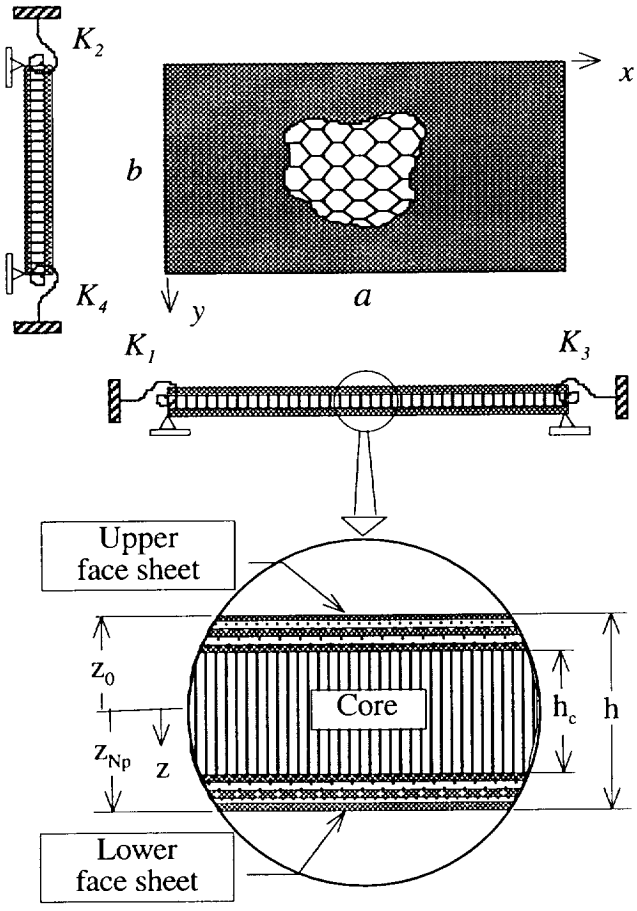

Figure 1. General description of the sandwich plate model

1.1 Reliability Analysis

The reliability is defined here as the probability that the panel will not buckle under the applied load. Mathematically, this statement can be expressed as

$$R_e = \mathrm{P}(\overline{N}_{cr} > \overline{N}_a) \tag{1}$$

In this context, the performance function that describes plate reliability is given as

$$Z = \overline{N}_{cr} - \overline{N}_a = g(\overline{X}) \tag{2}$$

where $\overline{X}$ is the vector of basic random variables affecting plate reliability, and $g(.)$ is a function that describes the relationship between the performance function and the basic random variables. Plate failure is defined by $Z < 0$; plate survival is defined by $Z > 0$; and the limit state is defined by $Z = 0$.

In advanced second-moment method (ASM) for calculating plate reliability, the basic random variables are transformed into a normalized coordinate system according to the relation

$$x'_i = \left(\overline{x}_i - \mu_{\overline{x}_i}\right) / \sigma_{\overline{x}_i} \quad \text{for } i = 1, 2, ..., n \tag{3}$$

The resulting normalized random variables have mean of zero and standard deviation of one (i.e., $\mu_{x'_i} = 0$ and $\sigma_{x'_i} = 1$). Based on ASM the shortest distance, in the reduced coordinate system, measured from the origin to the limit state ($Z = 0$) or failure surface defines the reliability index β also known as the Hasofer-and-Lind (HL) index.

The iterative procedure described by Ayyub and McCuen[3] is used here to calculate β. The plate reliability is then calculated using the relationship between β and the probability of failure given by

$$P_f = 1 - \Phi(\beta) = 1 - R_e \tag{4}$$

The decision on what reliability method to use followed an initial comparison between ASM and the first order reliability method (FORM). Although the latter is easier to implement, it was found to underestimate plate reliability mainly due to the non-linearity of the performance function. Hence, only ASM was used in reliability-based optimization.

1.2 Effectivity Analysis Based on Taguchi Method

In order to identify the statistically significant parameters affecting the buckling response of a sandwich plate, a design of experiments (DOE) was set up based on the principles of Taguchi method. Eleven main factors at two levels and four two-factor interactions were considered in the DOE. Using the L_{16} orthogonal array a total of sixteen experiments were conducted. The order of factors influencing the panel buckling strength is found to be h_c, t, t*h_c, **K**, t***K**, G_{12}, G_{zx}, θ, G_{yz}, ν, t*θ, E_2, E_1, (*a*/b)***K**, and *a*/b. The description of each parameter and its mean value are given in Table 1. Among all factors the face sheet ply thickness and the core thickness are found to have the most significant influence on the buckling load. Details of this investigation including the robust design configuration for buckling load maximization can be found in ref. 4.

Table 1. Description of basic random variables

Basic Random Variable	Mean	CoV, %	Distribution
axial load, N_x	2000 N/mm	2.5	Normal
axial load, N_{xy}	2000 N/mm	2.5	Normal
plate length, a	254 mm	5.0	Normal
plate width, b	254 mm	5.0	Normal
edge rotational stiffness along $y = 0$, b edges, $K = bK/D_{22}$	10	5.0	Normal
Face Sheets: graphite-epoxy			
ply thickness[a]	t_0, t_{45}, t_{-45}, t_{90}	5.0	Normal
ply angle[b]	0, 45, -45, 90	5.0	Normal
Young's modulus, E_1	229 GPa	2.5	Normal
Young's modulus, E_2	13.35 GPa	2.5	Normal
shear modulus, G_{12}	5.25 GPa	2.5	Normal
Poisson's ratio, ν_{12}	0.315	2.5	Normal
Core: aluminum honeycomb			
thickness[a]	h_c	5.0	Normal
shear rigidity, G_{xz}	0.146 GPa	2.5	Normal
shear rigidity, G_{yz}	0.0904 GPa	2.5	Normal

[a] design variables
[b]For the 0° ply a standard deviation of ±1° is used

1.3 Probabilistic Design Optimization

For the composite sandwich plate the probabilistic optimization problem is formulated as

$$\text{Min.} \quad f(\bar{X}, \bar{Y})$$

$$\text{s.t.} \quad \beta \quad \beta_{min} \qquad (5)$$

$$\bar{Y}^l \le \bar{Y} \le \bar{Y}^u$$

where the objective function f is the plate weight, $\bar{Y}$ is the vector of design variables, representing a subset of the random variable vector $\bar{X}$, defined in Table 1, and β_{min} is the required minimum reliability index which in this case is set to 3.09 for a reliability of 0.999. All random variables are assumed to have normal distributions with specified means and assumed coefficients of variation (CoV) given in Table 1.

Each face sheet is an unsymmetric quasi-isotropic laminate with four plies made of graphite-epoxy material. The sandwich plate is symmetric about its midplane surface. The mean values for ply and core thicknesses are treated as the only design variables in the optimization process. In the probabilistic design problem the performance function in Eq. (2) is approximated as

$$\mu_Z = \mu(\bar{N}_{cr}) - \mu(\bar{N}_a) \qquad (6)$$

with mean value of the buckling load obtained from the deterministic procedure described in ref. 1.

1.4 Deterministic Design Optimization

For the composite sandwich plate the deterministic optimization problem is formulated as

$$\begin{aligned} &\text{Min.} \quad f(\overline{X}, \overline{Y}) \\ &\text{s.t.} \quad \overline{N}_{cr} \geq FS\,(\overline{N}_a) \\ &\qquad \overline{Y}^l \leq \overline{Y} \leq \overline{Y}^u \end{aligned} \tag{7}$$

where the objective function f is the plate weight, and FS is the factor of safety against buckling. The design variables in this case are assumed to be deterministic. The design reliability is calculated for the optimal design as a post-optimization step.

1.5 Results and Discussion

The deterministic and probabilistic optimization problems are solved each for two different loading conditions (N_x and N_{xy}). In each case the bounds on design variables are: 0.0254 mm $< t_{ply} <$ 7.62 mm and 0.254 mm $< h_c <$ 16.51 mm. The face sheet material has a density of 1600 kg/m^3 while the honeycomb core has an effective density of 27.1 kg/m^3.

To demonstrate the effect of rotational edge stiffness, three different plate boundary conditions are considered. In the first case the plate is assumed to be simply supported, i.e., $\boldsymbol{K}_1 = \boldsymbol{K}_3 = \boldsymbol{K}_2 = \boldsymbol{K}_4 = 0$. In the second case the plate is simply supported at $x = 0$ and a edges but elastically restrained against rotation along the other two edges such that $\boldsymbol{K}_1 = \boldsymbol{K}_3 = 0$ and $\boldsymbol{K}_2 = \boldsymbol{K}_4 = 10$. In the last case, the rotational stiffness along $y = 0$, b edges is increased to infinity making those two edges clamped. For each case, the optimal design is obtained for three different aspect ratios (a/b=0.5, 1.0, and 2.0). The initial design for all cases is chosen as $t_0 = t_{45} = t_{-45} = t_{90} =$ 1.27 mm and h_c =15.24 mm.

The results of optimization are given in Tables 2 and 3. In all cases the core thickness is pushed near its upper bound. Since thickness has a large influence on plate bending stiffness, it is reasonable to see the core thickness increase. This increase in thickness causes the face sheets to move farther apart, therefore, increasing the plate bending stiffness D_{ij}.

However, a similar increase in thickness is not observed in the face sheet plies. This is because the density of face sheet plies is significantly higher than that of the core. Hence, increasing the face sheet thickness has a greater impact on the overall weight of the plate that is being minimized.

The thickness is seen to increase only in plies that offer greater support against buckling. For example, the contribution of the 90° plies against axial buckling is far less than the others. Therefore, we see this ply thickness remain near its lower bound value in almost all optimal designs.

The deterministic and probabilistic optimal designs for axial loading condition indicate the 0° plies to be the most dominant followed by -45° and 45° plies. For the positive shear loading case, however, the 45° plies are more dominant than the 0° plies. It is expected that for the negative shear loading the -45° plies would be the most dominant. There is also a greater balance between the ±45° plies in the axial than in the shear buckling case for all aspect ratios and support conditions investigated.

Table 2. Optimal design of (0°/±45°/90°/Core)$_s$ sandwich plates under uniaxial compression, N_x ($K_1 = K_3 = 0$; $K_2 = K_4 = bK/D_{22}$)

bk/D_{22}	t_0, mm	t_{45}, mm	t_{-45}, mm	t_{90}, mm	h_c, mm	Deterministic Design		Probabilistic Design	
						Reliability	Weight, gm	Reliability	Weight, gm
					a/b = 0.5, Area = 6.4516 x 10^{-2} m^2				
0	0.2750	0.0527	0.0537	0.0254	16.51	0.4920	112.84		
	0.5096	0.1683	0.0254	0.0254	16.50			0.9990	179.24
10	0.2798	0.0363	0.0365	0.0254	16.51	0.4920	106.90		
	0.4542	0.0876	0.0888	0.0254	16.51			0.9990	164.26
∞	0.2418	0.0342	0.0340	0.0254	16.51	0.4920	98.10		
	0.3808	0.0752	0.0766	0.0254	16.51			0.9990	144.04
					a/b = 1.0, Area = 6. 4516 x 10^{-2} m^2				
0	0.2594	0.1584	0.1613	0.0254	15.29	0.4920	151.49		
	0.4237	0.1562	0.1635	0.0271	16.33			0.9987	187.60
10	0.3297	0.0883	0.0929	0.0254	15.30	0.4880	137.46		
	0.4493	0.0887	0.0912	0.0254	16.48			0.9987	163.95
∞	0.2331	0.0421	0.0490	0.0254	16.36	0.4980	100.76		
	0.3810	0.0728	0.0785	0.0254	16.51			0.9990	143.97
					a/b = 2.0, Area = 6. 4516 x 10^{-2} m^2				
0	0.2382	0.1224	0.1262	0.0254	16.30	0.4880	134.255		
	0.4205	0.2199	0.2156	0.0271	16.08			0.9991	210.39
10	0.2578	0.0819	0.0869	0.0254	16.51	0.4900	121.09		
	0.3750	0.1656	0.1759	0.0254	16.37			0.9989	181.75
∞	0.2148	0.0694	0.0678	0.0254	16.50	0.4900	106.76		
	0.3404	0.1129	0.1169	0.0254	16.50			0.9990	151.77

The deterministic results indicate the axial loading to be a more severe condition than shear loading for all boundary conditions and aspect ratios. A similar trend is also observed in the probabilistic results with a few exceptions. The weight of the simply-supported plate under shear loading is found to be higher than that under axial loading for a/b = 1 and 2.

For both loading conditions, with a few exceptions, increasing plate aspect ratio (for a fixed plate area) causes the weight to increase. On the other hand increasing the rotational rigidity along the y = 0, b edges causes the weight to decrease due to an increase in plate's resistance against buckling.

With FS = 1.0 in Eq. (7), the reliability of each deterministic optimal design is found to be roughly 50%. The tolerance specified for buckling constraint in the optimization analysis is set at 0.001, and that is why in most cases the reliability is slightly less than 0.5. The reliability of each probabilistic optimal design, by contrast, is found to be at or near 0.999.

For comparison, the plate having bk/D_{22} = 10 and a/b = 1 was optimized for uniaxial compression with FS = 1.25. The optimal weight is found to be 385.71 gm which is approximately 180% higher than the corresponding case in Table 2. It is evident that the 25% increase in the factor of safety results in a substantial increase in the weight.

Additional details of this investigation can be found in ref. 5. Future investigation will focus on maximization of reliability index and factor of safety (for deterministic design). This approach will determine the conditions under which the reliability can be increased to its maximum for a specified plate weight.

Table 3. Optimal design of $(0°/\pm45°/90°/\text{Core})_s$ sandwich plates under uniform shear load, N_{xy} ($K_1 = K_3 = 0$; $K_2 = K_4 = bK/D_{22}$)

bk/D_{22}	t_0, mm	t_{45}, mm	t_{-45}, mm	t_{90}, mm	h_c, mm	Deterministic Design		Probabilistic Design	
						Reliability	Weight, gm	Reliability	Weight, gm
					a/b = 0.5, Area = 6. 4516 x 10^{-2} m^2				
0	0.0254	0.0386	0.0254	0.0254	16.51	0.5000	52.58		
	0.0548	0.0819	0.0254	0.0254	16.51			0.9987	67.58
10	0.0254	0.0257	0.0254	0.0254	16.51	0.4920	49.92		
	0.0372	0.0729	0.0254	0.0254	16.14			0.9989	61.42
∞	0.0254	0.0254	0.0254	0.0254	16.51	0.5199	49.84		
	0.0436	0.0566	0.0254	0.0254	16.51			0.9990	60.04
					a/b = 1.0, Area = 6. 4516 x 10^{-2} m^2				
0	0.0621	0.2578	0.0254	0.0254	16.51	0.4841	105.373		
	0.3518	1.0380	0.0254	0.0254	16.51			0.9990	326.22
10	0.0403	0.2066	0.0254	0.0254	16.51	0.4860	90.320		
	0.1073	0.4303	0.0254	0.0254	16.50			0.9988	150.29
∞	0.0358	0.1855	0.0254	0.0254	16.50	0.4860	85.000		
	0.1079	0.2945	0.0254	0.0761	16.50			0.9990	132.86
					a/b = 2.0, Area = 6. 4516 x 10^{-2} m^2				
0	0.0254	0.3817	0.0254	0.0254	16.51	0.4880	123.39		
	0.1545	1.0867	0.0254	0.0657	16.51			0.9990	303.88
10	0.0254	0.3555	0.0254	0.0254	16.51	0.4920	117.98		
	0.1189	0.7096	0.0254	0.0968	16.51			0.9989	225.09
∞	0.0254	0.2723	0.0254	0.0264	16.51	0.5000	100.99		
	0.0548	0.5383	0.0254	0.0690	16.51			0.9990	170.78

2. Global-Local Design of Damage Tolerant Structures

The second task in this research investigation involves the development of an efficient methodology for global-local analysis and optimization of damage-tolerant fuselage structures. The main focus areas are: (1) the application of strain energy density failure criterion, and (2) the development of response surface models for calculation of panel buckling load for use in global optimization.

The finite element method is used for the global analysis of the structure subject to a multidimensional loading condition as shown by the model in Fig. 2. The structure in Fig. 2 (a) represents the global model and the panel in Fig. 2 (b) represents the local model. The global model is assumed to be simply-supported at the ends with displacements restrained in radial and angular directions and free in the z direction. The local model is assumed to be simply-supported along all edges. The global structural model is to be optimized subject to constraints imposed on maximum strain energy density in each shell element, maximum stress in each bar element, and buckling of each panel.

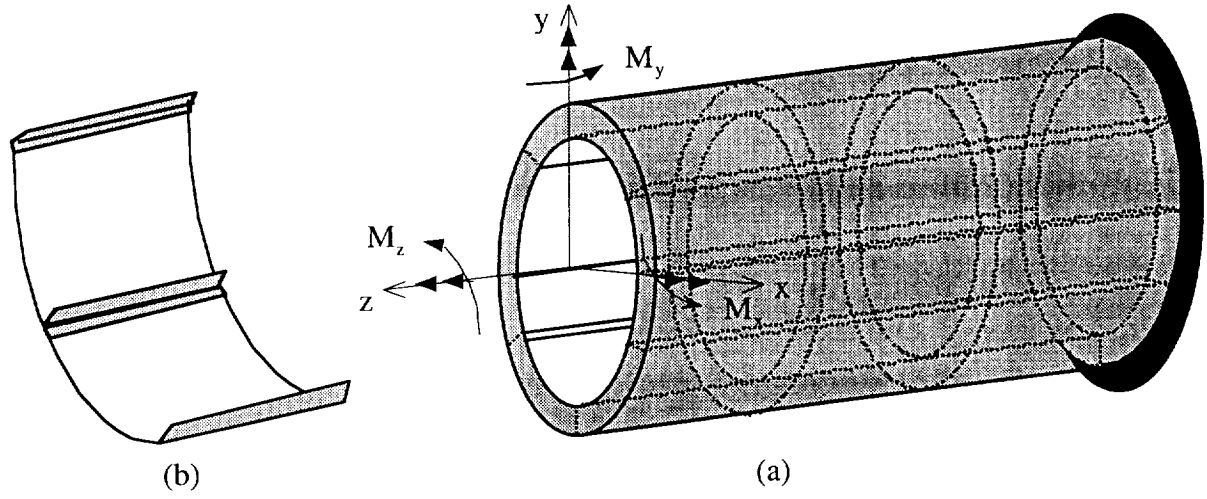

Figure 2. (a) Cylindrical fuselage section; (b) Stiffened panel

2.1 Strain Energy Density Failure Criterion

The strain energy density (SED) failure criterion, first proposed by Sih[6], is different from other classical fracture mechanics methods in that it does not require the presence of an initial flaw of known size and location. This criterion is based on the fact that strain energy stored in a material can be divided into dilatational and distortional parts, with failure initiation being associated with the dilatational part.

SED criterion identifies critical regions in the structure where the dilatational part of strain energy is the more dominant part. These regions are found to be susceptible to damage initiation and subsequent failure of the structure.

SED criterion of failure can be stated by the following two hypotheses[7]:

1) Failure is assumed to coincide at locations where the local minima of strain energy density function $(dW/dV)_{min}$ is at its maximum.

2) Failure initiation occurs when $(dW/dV)_{min}$ reaches its critical value governed by

$$\left(\frac{dW}{dV}\right)_c = \frac{S_1}{r_1} = \frac{S_2}{r_2} = - - - - = \frac{S_j}{r_j} = - - - - = \frac{S_c}{r_c} = const. \tag{8}$$

Where S_c is the critical strain energy density factor that serves as a measure of the fracture toughness value of the material and is found using

$$S_c = \frac{(1-2\nu)(1+\nu)}{2\pi(1-\nu^2)} G_{Ic} \tag{9}$$

where G_{Ic} is the critical energy release rate of the material and v is the Poisson's ratio. The unstable fracture begins when the ligament size reaches the critical value designated by r_c. G_{Ic} is related to the mode I stress intensity factor according to[8]

$$G_{Ic} = (1-\nu^2)\frac{K_{Ic}^2}{E} \tag{10}$$

where K_{Ic} is the critical stress intensity factor for mode I fracture of the material.

The SED criterion has been used for failure prediction in both isotropic and composite materials. In the case of laminated composite structures, it is used to obtain information on the onset of delamination[7]. In that case *r* represents the distance from the delamination front. The onset of unstable delamination is assumed to coincide with $(dW/dV)_{min}$ reaching its critical value.

Prior to the application of this criterion to the composite fuselage structure, it was tested on a 20" x 10 " x 0.5" aluminum rectangular plate with a 0.1" circular hole at the center. The plate is considered to be simply supported along exterior edges, and is under the action of uniform axial tensile force. Due to biaxial symmetry, one quarter of the plate, as shown in Fig. 3, is modeled for computational analysis. The model contains 120 four-noded quadrilateral shell elements with 882 degrees of freedom.

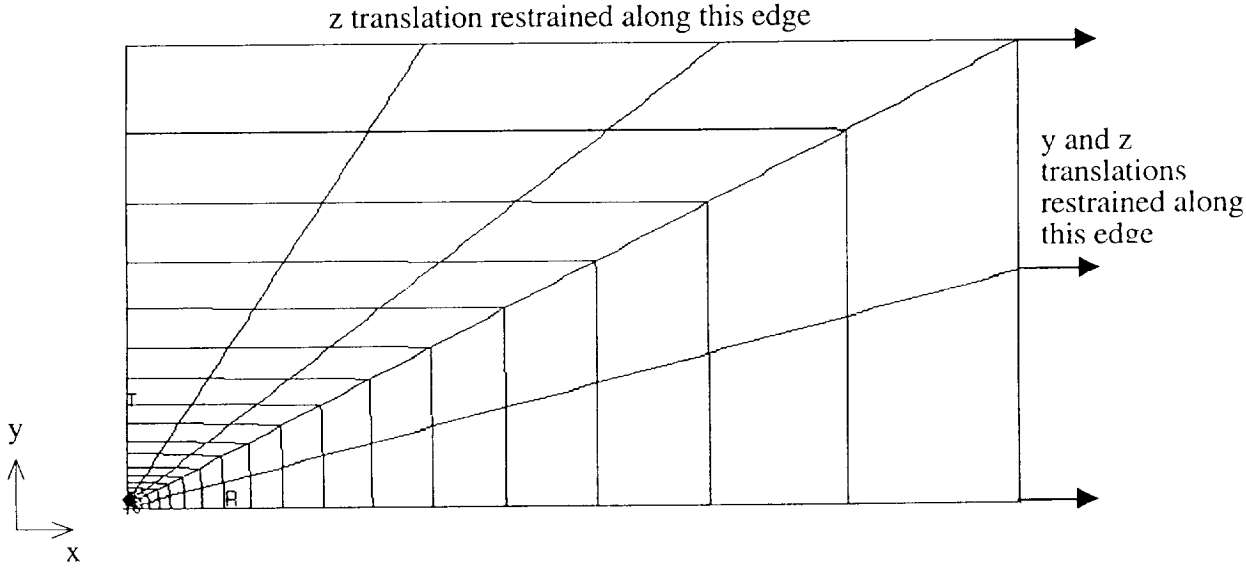

Figure 3. Finite element model of the plate with central circular hole

Symmetric boundary conditions are imposed along the axes of plate symmetry. The loaded edge is constrained against translation in the y and z directions while the unloaded edge is constrained only against translation in the z direction.

To determine the location of failure initiation, the strain energy density contours are first generated. Figure 4 shows the SED contours near the hole corresponding to the axial compressive load of 250 lb.

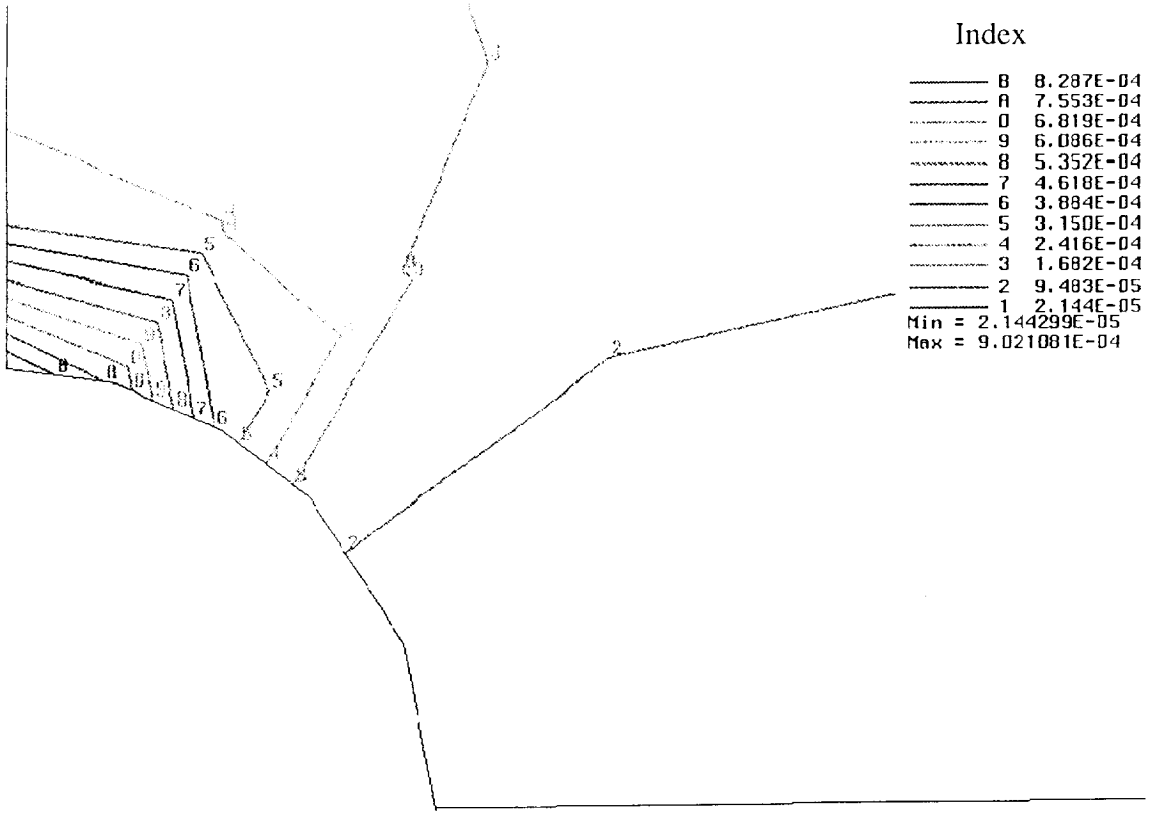

Figure 4. Strain energy density contours near the hole boundary

The variation of strain energy density along the boundary of the hole is plotted against angular position, θ in Fig. 5. Several distinct local minima of the strain energy density function are observed, among which the maximum occurs at $\theta = 78°$. Thus, we can conclude that failure will initiate at the point on the hole boundary which is at a 78° angle from the horizontal axis as shown in Fig. 6.

According to SED criterion the fracture propagation occurs in the direction where dW/dV reaches its critical value. In this case the local minima of dW/dV along various radius vectors centered at the point of fracture initiation need to be calculated. Thus three circles of radii $r_o = 0.005$ *in*, 0.010 *in*, 0.015 *in* are drawn. Using the plot of dW/dV versus θ, as shown in Fig. 7, the maximum

of $(dW/dV)_{min}$ is found to occur at approximately 50°. The direction of damage propagation is shown in Fig. 8.

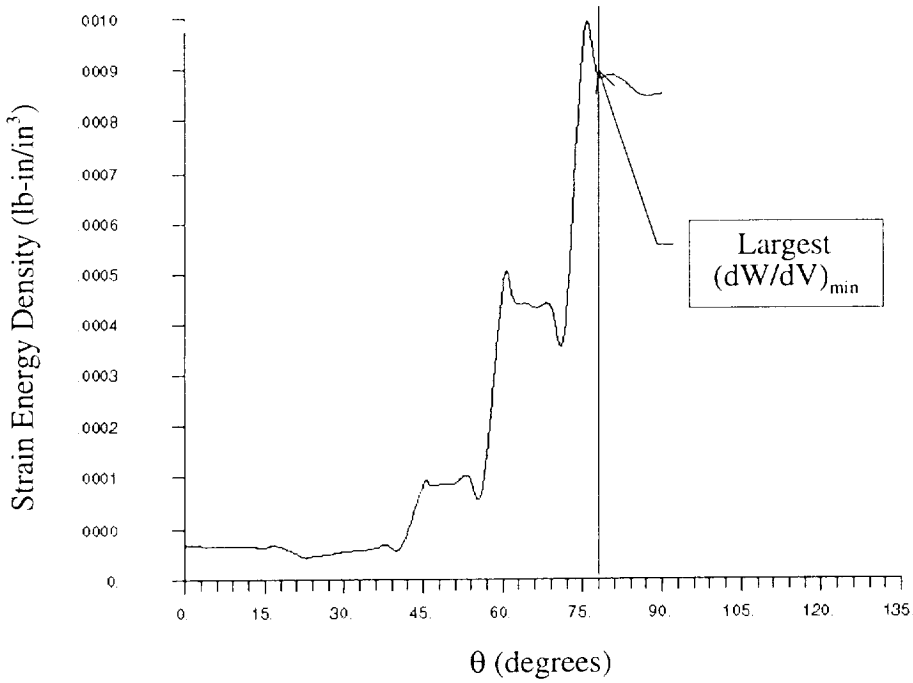

Figure 5. Strain energy density variation with angular position showing the location of failure initiation to be at 78°

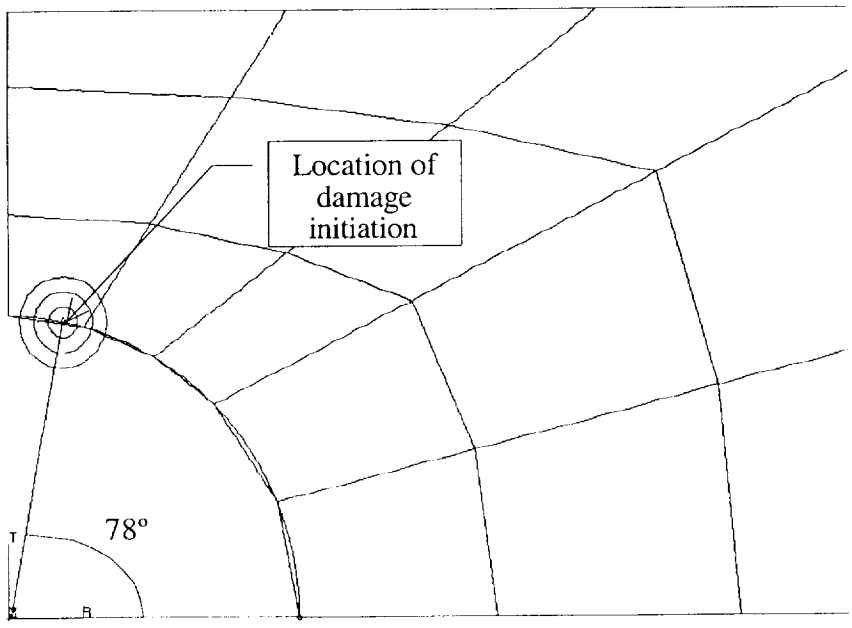

Figure 6. Point of failure initiation at the hole boundary

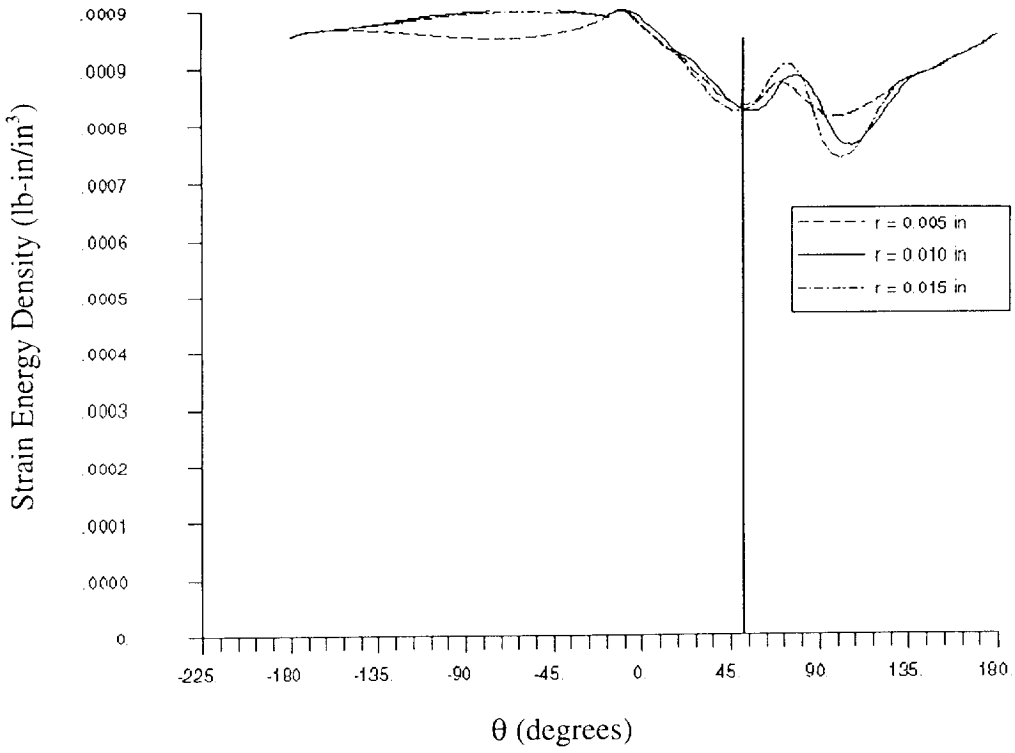

Figure 7. Strain energy density variation with angular position showing the direction of failure propagation to be around 50°

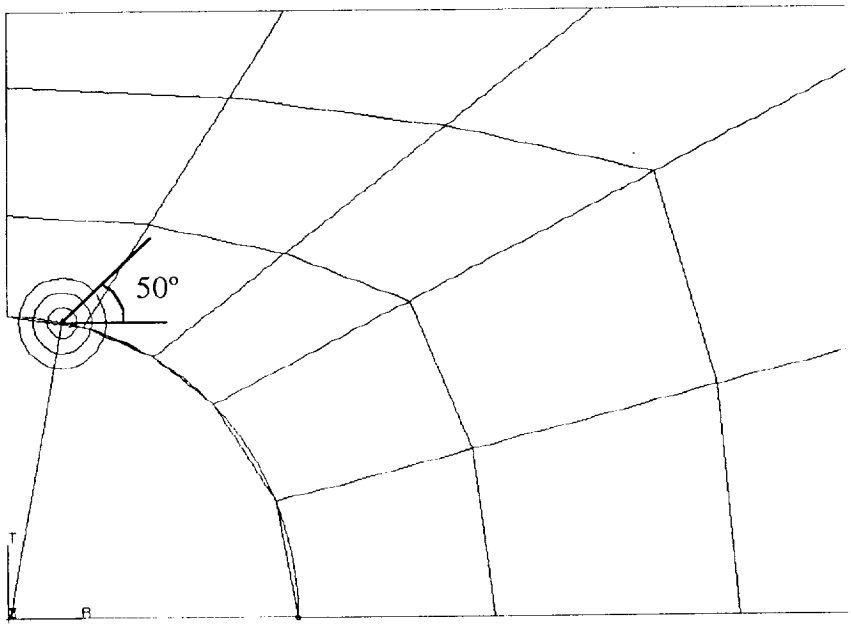

Figure 8. Direction of damage propagation

For damage tolerance consideration, a limit will be imposed on the strain energy density function to prevent it from exceeding the critical value associated with the material system used.

2.2 Response Surface Methodology

The use of finite element method for buckling analysis of a panel, representing a local model, in the optimization process of the global structural model would be very time consuming and inefficient. A more efficient alternative would be to use algebraic models derived from response surface methodology (RSM).

RSM uses mathematical and statistical techniques to generate algebraic equations for a particular response based on the specified set of variables or factors. For example, an RS model can be developed for estimating the buckling strength of a panel based on a set of geometric and/or stiffness variables.

Prior to applying this method to the composite fuselage structure, we applied it to the aluminum rectangular plate described in the previous section. The factors considered included the following geometric attributes: plate thickness, plate aspect ratio, and hole diameter. Since material variation was not considered, no stiffness parameters were included as independent factors.

The full factorial experiment (FFE) method is used to generate the response data. The FFE involving k factors with each having two levels is referred to as the 2^k design. With only three factors in this case, the FFE requires 8 (2^3) experiments. The experimental conditions are identified in Table 4. The low and high levels are denoted by –1 and 1, respectively. The low and high levels for these factors are as follows: plate thickness t = 0.5", 1", aspect ratio a/b = 1, 2, and hole diameter D = 0.1", 0.2". The loaded edge of the plate (b) is kept constant at 10".

Table 4. Experimental conditions and corresponding response values

Experiment	Treatment combinations	Design factors x_1, x_2, x_3	t, in	a/b	D, in	Buckling load (lb)
1	(1)	-1, -1, -1	0.5	1	0.1	5.0420E5
2	a	1, -1, -1	0.5	2	0.1	3.2795E6
3	b	-1, 1, -1	1	1	0.1	2.4930E5
4	ab	1, 1, -1	1	2	0.1	1.8129E6
5	c	-1, -1, 1	0.5	1	0.2	5.0260E5
6	ac	1, -1, 1	0.5	2	0.2	3.2765E6
7	bc	-1, 1, 1	1	1	0.2	2.4830E5
8	abc	1, 1, 1	1	2	0.2	1.8108E6

Since aspect ratio and hole diameter are geometric entities, any changes in them require the creation of a separate finite element model. In this case four different finite element models had to be created in order to account for low and high levels of aspect ratio and hole size. The finite-element based buckling load corresponding to each experimental condition is given in the last column of Table 4.

The effects of x_1, x_2, and x_3 are found as

$x_1 = (1/4)[a + ab + ac + abc - (1) - b - c - bc] = 2.1688E6$

$x_2 = (1/4)[b + ab + bc + abc - (1) - a - c - ac] = -0.8604E6$

$x_3 = (1/4)[c + ac + bc + abc - (1) - a - b - ab] = -1,925.0$

The two-factor interaction effects are found as

$x_1x_2 = (1/4)[abc - bc + ab - b - ac + c - a + (1)] = -0.6058E6$

$x_1x_3 = (1/4)[(1) - a + b - ab - c + ac - bc + abc] = -625.0$

$x_2x_3 = (1/4)[(1) + a - b - ab - c - ac + bc + abc] = 375.0$

and the three-factor interaction effect is found as

$x_1x_2x_3 = (1/4)[abc - bc - ac + c - ab + b + a - (1)] = 75.0$

Examining the magnitudes of the effects shows the plate thickness (x_1) to be the most dominant effect followed by aspect ratio (x_2) and the x_1x_2 interaction. The effect of hole size in this case is rather insignificant due to its small magnitude.

Based on the statistical analysis on the significance of each effect, a multiple linear regression model defined by

$$P'_{cr} = \beta_0 + \beta_1 x_1 + \beta_2 x_2 + \beta_{12} x_1x_2 + \varepsilon \tag{11}$$

is the simplest model that could be used to estimate the plate buckling load as the response of interest with ε representing the random error term. In this case the random error term is zero as computational simulations are used in place of physical experiments to generate the response data. Therefore, only the first four terms are of concern in Eq. (11). The regression coefficients β_1, β_2, and β_{12} are estimated by one half of the corresponding effect estimates, and β_0 is estimated by the average of the buckling loads in FFE. Thus,

$$P'_{cr} = 10^6 (1.4605 + 1.0844 x_1 - 0.4302 x_2 - 0.3029 x_1x_2) \tag{12}$$

is the response surface model for the plate buckling load with corresponding predicted values given in the fourth column of Table 5. The residual or difference between the finite-element based "actual" buckling loads and the estimated (fitted) values are shown in the last column of Table 5.

Table 5. Comparison of actual and estimated axial buckling loads

Experiment	Design factors x_1, x_2, x_3	FE solution, P_{cr}	FFE, P'_{cr}	Residual, $e = P_{cr} - P'_{cr}$	Standardized residual, d
1	-1, -1, -1	5.0420E5	5.0340E5	800	0.54928
2	1, -1, -1	3.2795E6	3.2780E6	1500	1.02990
3	-1, 1, -1	2.4930E5	2.4880E5	500	0.34330
4	1, 1, -1	1.8129E6	1.81185E6	1050	0.72093
5	-1, -1, 1	5.0260E5	5.0340E5	-800	-0.54928
6	1, -1, 1	3.2765E6	3.2780E5	-1500	-1.02990
7	-1, 1, 1	2.4830E5	2.4880E6	-500	-0.34330
8	1, 1, 1	1.8108E6	1.81185E6	-1050	-0.72093

A normal probability plot of the residuals is shown in Fig. 9. The residuals appear to fall along the "fat pencil" line indicating the normal distribution of the residuals.

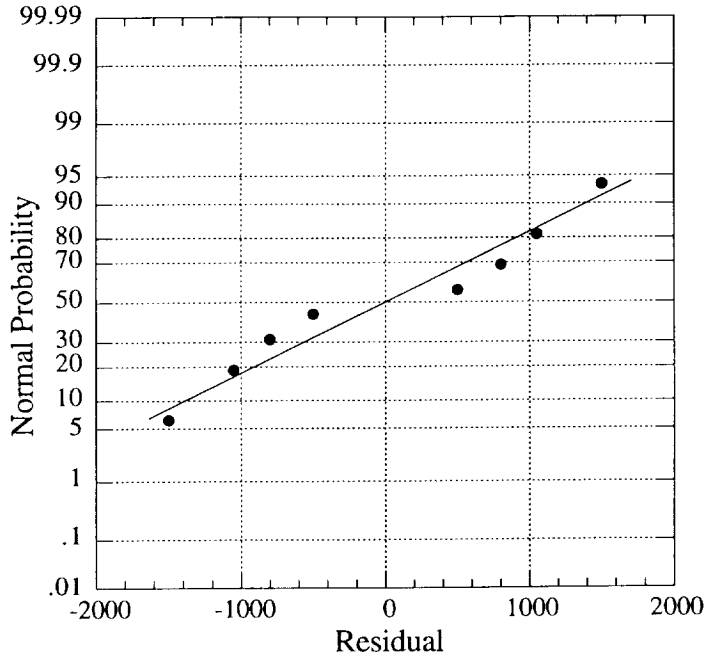

Figure 9. Normal probability plot of residuals associated with the regression model

The unbiased estimator of the residual variance σ^2 is determined as

$$\hat{\sigma}^2 = \frac{SS_E}{n-p} = \frac{\sum_{j=1}^{n=8} e_j^2}{8-4} = \frac{8.4850E6}{4} = 2.12125E6 \tag{13}$$

where SS_E is the sum of squares of the residuals, n is the number of experiments, and p is the number of terms in the regression model. The term n - p in the denominator of Eq. (13) represents the degrees of freedom associated with the residuals. With the estimator of the variance known, the standardized residuals are computed using

$$d_j = \frac{e_j}{\sqrt{\hat{\sigma}^2}}, \quad j = 1, 2, \cdots, n \tag{14}$$

with the values given in Table 5. Since all the computed standardized residuals fall in the interval of (-2, 2), the previously observed normal distribution of the residuals is reconfirmed.

Although the linear regression model appears to fit the response data fairly well, it does not represent the physics of the problem accurately. Looking at the buckling equation for an isotropic rectangular plate given as

$$\sigma_{cr} = k_c \frac{\pi^2 E}{12(1-\nu^2)}\left(\frac{t}{b}\right)^2 \tag{15}$$

indicates that buckling is a nonlinear function of plate thickness, with the aspect ratio affecting the buckling coefficient k_c. The nonlinearity of the response surface can be checked by calculating the response at the center point and comparing it with the average value of the responses at the low and high levels of thickness and aspect ratio. The finite element analysis of the plate at the center point corresponding to $x_1 = x_2 = x_3 = 0$ or t = 0.75", a/b = 1.5, and D = 0.15" gives the buckling load of approximately 1E6 lb. The average value for the buckling load at the four factorial points (x_1 = -1, 1, x_2 = -1, 1) is 1.46E6 lb. The difference of 46% indicates the presence of curvature at the center point. Therefore, in this case a second-order response surface described by the equation

$$P'_{cr} = \beta_0 + \beta_1 x_1 + \beta_2 x_2 + \beta_{11} x_1^2 + \beta_{22} x_2^2 + \beta_{12} x_1 x_2 \qquad (16)$$

should be considered as an alternative to the model in Eq. (11). The central composite design (CCD) is used in this case to design the experiments for generating the necessary response data. In CCD the complete or a fraction of 2^k factorial experiments are augmented with 2k axial runs at value of α for each factor and at least one center point. Therefore, for 2 factors, using the full factorial experiments would require at least 9 experiments. The experimental conditions are shown in Table 6. The zero level for each factor corresponds to the average value of –1 and 1. In this case α is set to 2. For thickness, levels -2 and 2 correspond to 0.25" and 1.25", respectively. For aspect ratio, levels –2 and 2 correspond to 0.5 and 2.5, respectively.

The estimated buckling loads at the new design points using Eq. (12) are given in the fourth column of Table 6. Unlike the estimates at the original design points, there are major discrepancies at most of the new design points.

Table 6. Comparison of actual and estimated axial buckling loads

Experiment	Design factors x_1, x_2, x_3	FE solution, P_{cr}	FFE, P'_{cr}	CCD, P'_{cr} (1 CP)	CCD, P'_{cr} (3 CP)	CCD, P'_{cr} (5 CP)
1	-1, -1, -1	5.0420E5	5.0340E5	5.022E5	4.899E5	4.861E5
2	1, -1, -1	3.2795E6	3.2780E6	3.167E6	3.155E6	3.151E6
3	-1, 1, -1	2.4930E5	2.4880E5	3.037E5	2.915E5	2.877E5
4	1, 1, -1	1.8129E6	1.81185E6	1.757E6	1.744E6	1.741E6
5	0, 0, 0	1.0000E6	1.46051E6	1.059E6	1.028E6	1.019E6
6	-2, 0, 0	4.0626E4	-7.0831E5	-141.25	5.991E3	7.894E3
7	2, 0, 0	4.0476E6	3.6293E6	4.117E6	4.124E6	4.125E6
8	0, -2, 0	2.3146E6	2.3209E6	2.357E6	2.363E6	2.365E6
9	0, 2, 0	7.6226E5	6.0014E5	7.487E5	7.548E5	7.567E5

The least squares method is used to estimate the unknown parameters in Eq. (16). The resulting second-order response surface equation is found to be

$$P'_{cr}|_{1CP} = 10^6 (1.059 + 1.029\ x_1 - 0.4022\ x_2 + \ 0.2499\ x_1^2 + \ 0.1235\ x_2^2 - 0.3029\ \ x_1 x_2) \qquad (17)$$

The estimated buckling loads using Eq. (17) are given in the fifth column of Table 6. As suggested by Montgomery and Runger[9], three to five central points are usually used to develop a response surface model. The response surface equations using three and five central points are found to be

$$P'_{cr}|_{3CP} = 10^6 (1.028 + 1.029\ x_1 - 0.4022\ x_2 + \ 0.2591\ x_1^2 + \ 0.1327\ x_2^2 - 0.3029\ \ x_1 x_2) \qquad (18)$$

$$P'_{cr}|_{5CP} = 10^6 (1.019 + 1.029\ x_1 - 0.4022\ x_2 + \ 0.2620\ x_1^2 + \ 0.1356\ x_2^2 - 0.3029\ \ x_1 x_2) \qquad (19)$$

with the corresponding point estimates given in Table 6. Since there is no random error in computational experiments, the additional central points result in the same values of response as those shown for the corresponding fifth experiment in Table 6. It is interesting to note that the inclusion of additional central points affected the values of β_0, β_{11}, and β_{22} but not the rest.

The mean square error MS_E or the unbiased estimator of the residual variance σ^2 for each of the CCD-based models is determined using

$$MS_E = \hat{\sigma}^2 = \frac{SS_E}{n-p} = \frac{\sum_{j=1}^{n} e_j^2}{n-6} \tag{20}$$

For one-, three-, and five-central point designs, the value of n is 9, 11, and 13, respectively. The corresponding $\hat{\sigma}^2$ is found to be 1.02285E10, 6.80391E9, and 4.98889E9 for one, three, and five central points, respectively. Using Eq. (14) the standardized residuals for each level of the CCD-based models are computed with the values shown in Table 7.

Table 7. Comparison of actual and estimated axial buckling loads

Experiment	Design factors x_1, x_2, x_3	FE solution, P_{cr}	Stan. residuals (1 CP)	Stan. residuals (3 CP)	Stan. residuals (5 CP)
1	-1, -1, -1	5.0420E5	0.01978	0.17336	0.25626
2	1, -1, -1	3.2795E6	1.11237	1.50935	1.81929
3	-1, 1, -1	2.4930E5	-0.53789	-0.51160	-0.54366
4	1, 1, -1	1.8129E6	0.55272	0.83530	1.01795
5	0, 0, 0	1.0000E6	-0.58337	-0.33945	-0.26900
6	-2, 0, 0	4.0626E4	0.40309	0.41989	0.46342
7	2, 0, 0	4.0476E6	-0.68621	-0.92622	-1.09582
8	0, -2, 0	2.3146E6	-0.41924	-0.58677	-0.71356
9	0, 2, 0	7.6226E5	0.13408	0.09044	0.07872

The standardized residuals for all three cases fall in the interval of (-2, 2). This implies that the errors are normally distributed and that there are no outliers. The comparison of the standardized residuals corresponding to each experiment shows the quadratic response surface model based on a single center point to be better than the other two. However, using the root mean square error $(MS_E)^{0.5}$ as the key indicator identifies the regression with five center points (5 CP) to have the best fit.

Another statistic that can be used to determine the quality of fit is the adjusted coefficient of multiple determination defined as

$$R_{adj}^2 = 1 - \left(\frac{n-1}{n-p}\right)\frac{SS_E}{S_{yy}} \tag{21}$$

where SS_E denotes the sum of squares of the residuals, and S_{yy} is the total corrected sum of squares of observations (P_{cr}). Based on the data in Table 6, R^2_{adj} for the 1 CP, 3 CP, and 5 CP models are found to be 0.99484, 0.99480, and 0.99642, respectively. While there is very little difference between the R^2_{adj} values, the 5 CP model appears to fit the data better.

In the coming year we plan to incorporate both the strain energy density failure criterion and the response surface methodology in the design of composite fuselage structure. In that case the local buckling load would be captured via the response surface equation and the strain energy density criterion will help introduce a damage tolerance constraint in the global optimization problem.

References

1. Marcellier, P. and Rais-Rohani, M., "Free Vibration and Buckling Analysis of Anisotropic Sandwich Plates With Edges Elastically Restrained Against Rotation," Proceedings of the 39th AIAA/ASME/ASCE/AHS/ASC Structures, Structural Dynamics and Materials Conference, Long Beach, CA, April 20-23, 1998, Part 4, pp. 3185-3200.

2. DOT optimization software, Vanderplaats Research and Development, Inc. 1995.

3. Ayyub, B.M. and McCuen, R.H., Probability, Statistics, and Reliability for Engineering, CRC Press, New York, 1997, pp. 404-408.

4. Deo, S.K., Reliability-Based Design of Composite Sandwich Plates with Non-Uniform Boundary Conditions, M.S. Thesis, Department of Aerospace Engineering, Mississippi State University, May 1999.

5. Deo, S.K. and Rais-Rohani, M., "Reliability-Based Design of Composite Sandwich Plates with Non-Uniform Boundary Conditions," Proceedings of the 40th AIAA/ASME/ASCE/AHS/ASC Structures, Structural Dynamics and Materials Conference, St. Louis, MO, April 12-15, 1999. Paper no. AIAA-99-1580.

6. Sih, G.C., Mechanics of Fracture Initiation and Propagation, Kluwer Academic Publishers, Dordrecht, 1991.

7. Persson, E., Madenci, E., and Eriksson, I., "Delamination Initiation of Laminates with Pin-Loaded Holes," *Theoretical and Applied Fracture Mechanics*, Vol. 30, 1998, pp. 87-101.

8. Broek, D., Elementary Engineering Fracture Mechanics, 4th Ed., Kluwer Academic Publishers, Dordrecht, 1996.

9. Montgomery, D.C., and Runger, G.C., Applied Statistics and Probability for Engineers, John Wiley & Sons, Inc., New York, 1994.